JOURNAL OF APPLIED ELECTROCHEMISTRY 15 (1985) 447–451

# *Oxide ion and electron mixed conduction in the fluorite-type cubic solid solution in the system $Bi_2O_3$–$Tb_2O_{3.5}$*

T. ESAKA, H. IWAHARA

*Department of Environmental Chemistry and Technology, Faculty of Engineering, Tottori University, Minami 4-101, Koyama-cho, Tottori, 680 Japan*

Received 3 September 1984

Electrical conduction in sintered oxides of the system $Bi_2O_3$–$Tb_2O_{3.5}$ has been investigated. Oxide ion conduction was observed in the rhombohedral (low temperature) phase and the f c c (high temperature) phase present in the composition range less than 20 mol % $Tb_2O_{3.5}$. The f c c phase could be stabilized at lower temperatures by adding more than 30 mol % $Tb_2O_{3.5}$. In addition to oxide ion conduction, appreciable electronic conduction appeared in this composition range. The oxide ion transport number of this phase decreased with increasing content of $Tb_2O_{3.5}$ and the specimens having 40–50 mol % $Tb_2O_{3.5}$ showed mixed conduction where electrical conduction was comparably contributed by oxide ions and electrons. Electronic conduction in the f c c phase was considered to be due to the change in valence of terbium at high temperatures.

## 1. Introduction

A highly conductive mixed conductor in which both oxide ions and electrons transport electricity in a single phase would have a potential use as an electrode material for fuel cells [1, 2] and as a diaphragm for extraction of pure oxygen from air. We are currently investigating conductors suitable for these purposes.

On the other hand, we have also studied highly conductive oxide ion conduction in the sintered oxides based on $Bi_2O_3$. The high temperature δ-form (fluorite-type face centred cubic) of $Bi_2O_3$ which shows high oxide-ion conduction was stabilized by adding some special oxides such as $Y_2O_3$, $Gd_2O_3$, $Nb_2O_5$ etc; the resulting phase showed high oxide ion conductivity at lower temperatures [3–7]. Those oxides were not good electronic conductors because the oxide dopants such as $Y_2O_3$, $Gd_2O_3$ or $Nb_2O_5$ do not change their oxidation state to form conduction electrons under ordinary oxygen atmospheres. If $Bi_2O_3$ is doped by an oxide whose cation has an appropriate ionic radius and an easily changed oxidation state, we can expect not only stabilization of the δ-form, but also oxide ion and electron mixed conduction due to the change of valence. $Pr_6O_{11}$ and $Tb_4O_7$ are considered to be suitable for such an oxide dopant. As previously reported, we found that the LaOF-type rhombohedral phase in the system $Bi_2O_3$–$Pr_2O_{11/3}$ was such a mixed conductor [8]. As to the system $Bi_2O_3$–$Tb_4O_7$, there were a few brief reports concerning the electrical conduction and the crystal phase [9, 10]. However, they did not refer to the mixed conduction in these materials. Therefore, the authors have studied the mixed electrical conduction in the sintered oxides of the system $Bi_2O_3$–$Tb_2O_{3.5}$.

## 2. Experimental details

### *2.1. Preparation of specimens*

The specimens were prepared from $Bi_2O_3$ (special grade by Kanto Chem. Co.) and $Tb_4O_7$ (99.9%). In the following studies we take the expression $Tb_2O_{3.5}$ instead of $Tb_4O_7$ to match the cation number with that of $Bi_2O_3$. These materials were weighed in a defined molar ratio, mixed in an agate mortar, and fired at 800–1200° C in air for

0021-891X/85 $03.00 + .12 

10 h. The firing temperature was raised with increasing $Tb_2O_{3.5}$ concentration in the specimen. The fired oxides were ground, pressed hydrostatically (2 ton $cm^{-2}$) into rods (5 mm $\phi$ by 5–10 mm length) or disks (12 mm $\phi$ by 2–3 mm thick), and sintered again under the same condition as that for the first firing. X-ray diffraction was carried out using Cu$K\alpha$-radiation to identify the crystal phase of the specimens prepared. These specimens were cooled slowly (about 2° C $min^{-1}$) from sintering temperature to room temperature to avoid freezing of the high temperature forms. In the special case to check a high temperature modification, the specimen was quenched from the sintering temperature to room temperature by blowing cold air over it.

### *2.2. Measurement of ionic conduction*

Electrical conductivity of specimens was obtained by measuring their impedance using a universal a.c. bridge with a 10 kHz signal. Rod specimens were generally employed in this measurement. Platinum powder paste was smeared on both ends of the rod samples and fired to serve as the electrodes.

The ionic transport number of specimens was determined from the e.m.f. of an oxygen gas concentration cell constructed using a disk specimen as the electrolyte. Air at 1 atm and oxygen gas were used as the anode and cathode gas, respectively. If the conduction in the specimen is purely ionic, the e.m.f. $E_0$ of the cell

$$\text{Gas I } (P_{O_2,a}), \text{ Pt/specimen disk/Pt, Gas II } (P_{O_2,c}) \quad (1)$$

is given by Equation 2

$$E_0 = (RT/4F) \ln [(P_{O_2,c})/(P_{O_2,a})] \quad (2)$$

where $R$, $T$ and $F$ have their usual meanings. In an ion and electron mixed conductor the e.m.f. $E$ is lowered from $E_0$. In such a case, the ratio of the ionic conductivity $\sigma_i$ to the total conductivity $\sigma_t$, that is , the ionic transport number $t_i$, can be given by the following equation if the electrode reaction is sufficiently reversible;

$$t_i = \sigma_i/\sigma_t = \sigma_i/(\sigma_i + \sigma_e) = E/E_0 \quad (3)$$

where $\sigma_e$ is the electronic conductivity.

Ionic conduction was also investigated by measuring the conductivity under various oxygen pressures. In general, the conductivity of an oxide conductor is represented by the following equation,

$$\sigma = \sigma_o + \sigma_p P_{O_2}^{1/n} + \sigma_n P_{O_2}^{-1/n} \quad (4)$$

where $\sigma_o$ is the oxide ion conductivity, $\sigma_p$ and $\sigma_n$ are constants related to hole and excess electron conductivities, respectively, and $P_{O_2}$ is the partial pressure of oxygen equilibrated with the oxide conductor. Therefore, the type of conduction is presumed from the dependence of conductivity on $P_{O_2}$.

## 3. Results and discussion

### *3.1. The crystal phase formed*

Fig. 1 shows X-ray diffraction patterns of the representative annealed specimens in the system $Bi_2O_3$–$Tb_2O_{3.5}$. Pure $Bi_2O_3$ shows the monoclinic crystal system ($\alpha$-$Bi_2O_3$). The specimens including less than 10 mol% $Tb_2O_{3.5}$ were mixed-phase with $\alpha$-$Bi_2O_3$ and an unknown. For the 20 mol% $Tb_2O_{3.5}$ specimen, the $\beta$-type rhombohedral single phase was observed [11–13]. However, the formation range was so narrow that diffraction lines showing the coexistence of another phase were observed in the composition of 25 mol% $Tb_2O_{3.5}$. The specimen having more than 30 mol% $Tb_2O_{3.5}$ showed the fluorite-

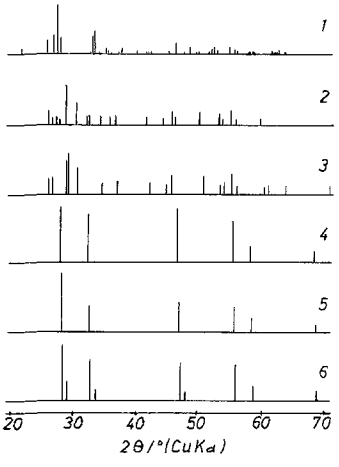


Fig. 1. X-ray diffraction patterns of $(Bi_2O_3)_{1-x}(Tb_2O_{3.5})_x$ annealed from sintering temperature to room temperature. (1) $x = 0.0$; (2) $x = 0.1$; (3) $x = 0.2$; (4) $x = 0.3$; (5) $x = 0.5$; (6) $x = 0.6$.

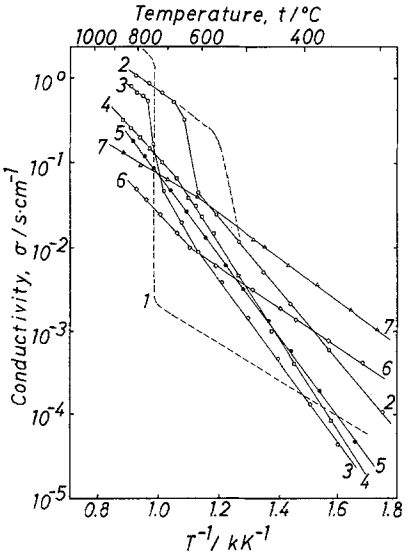


Fig. 2. Arrhenius plots of conductivity for sintered oxides of $(Bi_2O_3)_{1-x}(Tb_2O_{3.5})_x$. (1) $x = 0.0$; (2) $x = 0.1$; (3) $x = 0.2$; (4) $x = 0.3$; (5) $x = 0.4$; (6) $x = 0.5$; (7) $x = 0.6$.

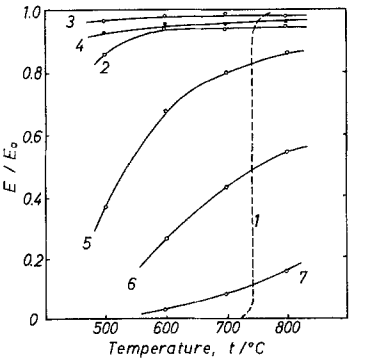


Fig. 3. $E/E_0$ versus temperature variations for the cell, $P_{O_2}$, a, $Pt/(Bi_2O_3)_{1-x}(Tb_2O_{3.5})_x/Pt$, $P_{O_2}$, c where $P_{O_2}$, a = 0.21 atm and $P_{O_2}$, c = 1.0 atm. (1) $x = 0.0$; (2) $x = 0.1$; (3) $x = 0.2$; (4) $x = 0.3$; (5) $x = 0.4$; (6) $x = 0.5$; (7) $x = 0.6$.

type cubic (f c c) phase. With increasing content of $Tb_2O_{3.5}$ each peak for the cubic phase was shifted toward a higher angle. Thus, the solid solution formation range of this f c c phase extends from 30 mol% to 50 mol% $Tb_2O_{3.5}$, and another phase based on $Tb_4O_7$ appears in the specimens containing more than 55 mol% $Tb_2O_{3.5}$.

On the other hand, quenched samples showed X-ray diffraction patterns corresponding to the f c c phase in the whole composition range investigated.

### 3.2. Conductivity

Arrhenius plots of the conductivity of $(Bi_2O_3)_{1-x}(Tb_2O_{3.5})_x$ are presented in Fig. 2 for the representative compositions. Pure $Bi_2O_3$ shows a conductivity jump at 730° C where the phase transition from the monoclinic to the f c c system takes place. The specimens of $x = 0.10$ and $x = 0.20$ showed similar conductivity jumps. The results of X-ray diffraction and differential thermal analysis indicated that the conductivity jump in these samples was also due to a phase transition from a low temperature form to the high temperature f c c phase. When more than 30 mol% $Tb_2O_{3.5}$ was added and the high temperature f c c phase was stabilized at lower temperatures, the conductivities showed almost linear variations over the wide range of temperatures measured. The special conductivity break in the sample of $x = 0.50$ is discussed below.

### 3.3. Conduction properties

Fig. 3 shows the $E/E_0$ versus temperature relationships. The sample of $x = 0.20$ showed values near unity over the temperature range examined. Steady and stable current could be drawn from the oxygen concentration cell indicating that the conduction in the oxide specimen can be ascribed to oxide ions. These results show that the rhombohedral phase as well as the f c c phase is an oxide ion conductor. At $x = 0.3$, where the f c c phase is stable over a wide range of temperature, the conduction is also predominanly ionic. However, in the specimens with $x > 0.3$, $E/E_0$ values decreased with increasing content of Tb, indicating that electrons obviously participate in the conduction as the content of terbium increases. Electronic conduction is predominant in the 60 mol% $Tb_2O_{3.5}$ sample ($t_i < 0.2$).

Fig. 4 shows the dependence of conductivity on oxygen partial pressure for the representative specimens of $(Bi_2O_3)_{1-x}(Tb_2O_{3.5})_x$ at 800° C. In the case of $x = 0.2$, the conductivity was constant irrespective of $P_{O_2}$ indicating that electronic conduction is not predominant compared to ionic conduction. In the case of $x = 0.4$ and $x = 0.5$, however, the conductivity decreased with

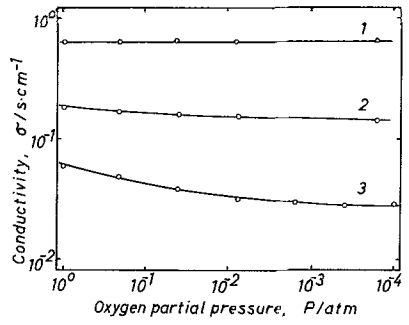


Fig. 4. $P_{O_2}$ dependence of conductivities for $(Bi_2O_3)_{1-x}(Tb_2O_{3.5})_x$ at 800° C. (1) $x = 0.2$; (2) $x = 0.4$; (3) $x = 0.5$.

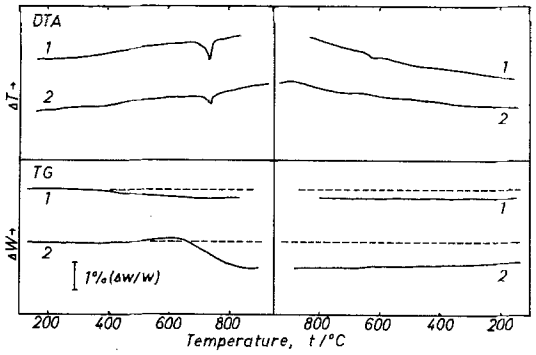


Fig. 6. DTA and TG results for $(Bi_2O_3)_{1-x}(Tb_2O_{3.5})_x$ in air. (1) $x = 0.1$; (2) $x = 0.4$.

decreasing $P_{O_2}$. This suggests that electronic conduction due to electron holes takes part in these specimens. Ionic transport numbers in air were calculated from these variations assuming that the conductivity at lower $P_{O_2}$ shows pure ionic conductivity. The values were 0.85 and 0.58 for $x = 0.40$ and 0.50, respectively, which coincided with the values calculated from the e.m.f.'s of the $O_2$-air concentration cell.

Fig. 5 shows Arrhenius plots of ionic ($\sigma_i$) and electronic conductivity ($\sigma_e$) of the typical samples. These values were obtained from the results of conductivities and ionic transport numbers mentioned above; $\sigma_i$ decreases and $\sigma_e$ increases with increasing content of terbium. The activation energy for oxide ion conduction was obviously different from that for electronic conduction. The apparent conductivity break in the $x = 0.5$ specimen in Fig. 2 is attributed to the intersection of the $\sigma_i$ and $\sigma_e$ lines on the Arrhenius plots.

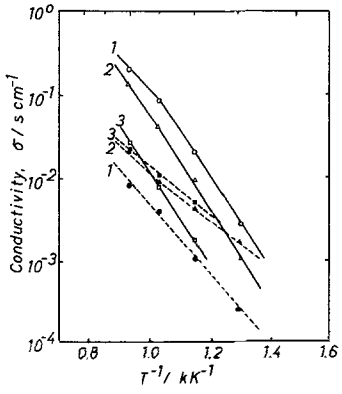


Fig. 5. Arrhenius plots of ionic (solid line) and electronic conductivity (broken line) for $(Bi_2O_3)_{1-x}(Tb_2O_{3.5})_x$. (1) $x = 0.3$; (2) $x = 0.4$; (3) $x = 0.5$.

Terbium is considered to contribute to the formation of electron holes. Therefore, we investigated the change in the valence of terbium at high temperatures by thermal analysis. Fig. 6 shows typical DTA and TG results. During heating of the mixed powders of the starting oxides ($Bi_2O_3$ and $Tb_2O_{3.5}$) nothing was observed except an endothermic peak on the DTA chart due to the phase transition of $Bi_2O_3$ at above 730° C, whereas the weight loss of the sample was recorded at about 400° C on the TG chart. Quantitative analysis of the change in weight showed that Tb finally became trivalent at high temperatures. As pure terbium oxide ($Tb_2O_{3.5}$) showed no weight loss during heating, $Bi_2O_3$ as the host material was considered to make Tb trivalent. Therefore, the oxide system can be represented as $(Bi_2O_3)_{1-x}(Tb_2O_3)_x$. In this case oxide ion vacancies are present in the specimens as reported in other systems [3, 4]. However, during cooling, the sample containing comparatively much Tb ($x = 0.4$) showed an increase in weight due to the increase of oxygen content. These phenomena suggest that the oxide ion vacancies are partly occupied by oxygen and that the hole conduction is caused as shown in the following equation

$$V_o^{\cdot\cdot} + 1/2\,O_2 \rightarrow O_O + 2h^+ \qquad (5)$$

At any rate, we found that the fluorite-type cubic phase can be a mixed conductor if it contained a large amount of terbium. This result is different from that for the system $Bi_2O_3$–$Pr_2O_{11/3}$ where the mixed conduction phase is the LaOF-type rhombohedral one in the composition range 40–50 mol% $Pr_2O_{11/3}$ [8]. The difference in the crys-

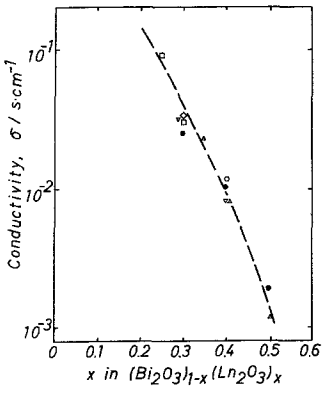


Fig. 7. Isothermal conductivity in the f c c phase of the system $(Bi_2O_3)_{1-x}(Ln_2O_3)_x$. (○) Ln = Sm; (△) Ln = Gd; ( ) Ln = Dy; (□) Ln = Er; (◇) Ln = Yb; (●) Ln = Tb.

tal structure results from the difference between the cationic radii of the doping oxides ($r^{3+}_{Pr}$ = 0.114 nm and $r^{3+}_{Tb}$ = 0.104 nm, Shannon and Prewitt [14]. As reported previously, the system $Bi_2O_3$–$Ln_2O_3$ (Ln = lanthanoid element) tends to crystallize in the δ-form (f c c) when $Ln^{3+}$ has a smaller ionic radius than that of $Sm^{3+}$ (0.109 nm) [15].

Oxide ion conducting f c c phases in the other systems $Bi_2O_3$–$Ln_2O_3$ have been previously reported [15]. We compared the oxide ion conductivities ($\sigma^{2-}_O$, calculated from $\sigma t_i$) of the cubic phase in the present system with those of the other systems. Fig. 7 indicates the relationship between oxide ion conductivities and $Ln_2O_3$ content at 600° C. As is seen from this figure, the plots of ionic conductivities vs the content of $Ln_2O_3$ lie on a general line [15] that includes the case of $Tb_2O_3$. This shows that the oxide ion conductivity of the f c c phase in the $Bi_2O_3$–$Ln_2O_3$ systems depends only on the composition irrespective of the kind of Ln.

## 4. Conclusion

In the system $Bi_2O_3$–$Tb_2O_{3.5}$ two kinds of single phase are observed. One is a β-type rhombohedral phase around the composition of 20 mol % $Tb_2O_{3.5}$ and the other is the fluorite-type cubic (f c c) phase in 30–50 mol % $Tb_2O_{3.5}$. In the former, oxide ion conduction is predominant and electronic conduction is negligibly low under an ordinary atmosphere. In the latter, electronic conduction is obviously observed in addition to oxide ion conduction, and the ionic transport number decreases with increasing content of $Tb_2O_{3.5}$. The electronic conduction is due to electron holes. As the valence of Tb and, hence, the concentration of oxygen vacancies in the crystal are readily changed in the f c c phase, hole conduction is considered to appear at comparatively high oxygen pressures. The specimen containing about 50 mol % $Tb_2O_{3.5}$ is a mixed conductor in which oxide ions and electron holes take part to the same extent.

## Acknowledgement

The authors gratefully acknowledge the support in part by a grant in aid of Scientific Research of the Ministry of Education, Science and Culture, Japan.

## References

[1] C. S. Tedson Jr, H. S. Spacil and S. P. Mitoff, *J. Electrochem. Soc.* **116** (1969) 1170.
[2] T. H. Etsell and S. N. Flengas, *Chem. Rev.* **70** (1970) 339.
[3] T. Takahashi, H. Iwahara and T. Arao, *J. Appl. Electrochem.* **5** (1975) 187.
[4] T. Takahashi, T. Esaka and H. Iwahara, *J. Appl. Electrochem.* **5** (1975) 197.
[5] *Idem, ibid. J. Appl. Electrochem.*, **7** (1977) 303.
[6] T. Takahashi, H. Iwahara and T. Esaka, *ibid.* **124** (1977) 1563.
[7] M. J. Verkerk, K. Keizer and A. J. Burggraaf, *ibid.* **10** (1980) 81.
[8] T. Esaka, H. Iwahara and H. Kunieda, *ibid.* **12** (1982) 235.
[9] R. K. Datta and J. P. Meehan, *Z. Anorg. Allg. Chem.* **383** (1971) 328.
[10] H. T. Cahen, T. G. M. Van Den Belt, J. H. W. De Wit and G. H. J. Broers, *Solid State Ionics* **1** (1980) 411.
[11] L. S. Sillen and B. Aurivillius, *Z. Crist.* **101** (1939) 483.
[12] J. C. Boivan and D. J. Thomas, *Solid State Ionics* **3/4** (1981) 457.
[13] P. Conflant, J. C. Boivan and D. J. Thomas, *J. Solid State Chem.* **35** (1980) 192.
[14] R. D. Shannon and C. T. Prewitt, *Acta Crystallogr.* **B25** (1969) 925.
[15] H. Iwahara, T. Esaka, T. Sato and T. Takahashi, *J. Solid State Chem.* **39** (1981) 173.